International Journal of Mechanical, Industrial and Aerospace Sciences
ISSN: 2517-9950
Vol:9, No:9, 2015

Effect of Welding Parameters on Penetration and Bead Width for Variable Plate Thickness in Submerged Arc Welding

Harish K. Arya, Kulwant Singh, R. K. Saxena

***Abstract*—**The heat flow in weldment changes its nature from 2D to 3D with the increase in plate thickness. For welding of thicker plates the heat loss in thickness direction increases the cooling rate of plate. Since the cooling rate changes, the various bead parameters like bead penetration, bead height and bead width also got affected by it. The present study incorporates the effect of variable plate thickness on penetration and bead width. The penetration reduces with increase in plate thickness due to heat loss in thickness direction for same heat input, while bead width increases for thicker plate due to faster cooling.

***Keywords*—**Submerged arc welding, plate thickness, bead geometry, cooling rate.

I. Introduction

RAPID heating and slow cooling during welding significantly affect the properties of weldment such as bead geometry, microstructural and mechanical strength. Because of local heating during welding process, controlling the thermal cycles is critical. Microstructure and micro-hardness are depending on the cooling rate which depends on the heat input controlled by process parameters. In present work, submerged arc welding is used because of capability to weld thicker sections, high quality, deep penetration than other processes [4]. The amount of heat input to the weld metal increases as voltage or current/wire feed rate or both increased. The heat input decreases with increase in welding speed [5]. The cooling rate of weldment decreases by increasing in heat input [6]. For the present study the combined effect of process parameters on bead geometry with variable plate thickness is investigated. Half fraction Central composite (rotatable) design is used for determining the relation between the process parameters and bead geometry of weldment and their relation with change in plate thickness.

II. Literature Survey

Several researchers in the past tried to establish relationship between bead geometry parameters and input variables of SAW and other welding processes [1], [2]. Mathematical model using fractional factorial design has been developed to predict weld bead geometry and shape relationship for GMAW welded AA 7005 plates [3]. Effect of heat input on bead geometry of Saw welded A 709 grade 50 material is studied and it is found that bead reinforcement, bead width, penetration, HAZ size, deposition area and penetration area increased with increasing heat input but the bead contact angle decreases with it [4]. Half fractional factorial design to develop a relationship between bead geometry, HAZ size parameters and polarity along with various welding parameters have been studied and it was found that effect of various process variables on heat flow follows similar trends for DCEP & DCEN slightly on lesser side of electrode negative. Narrower bead width and higher HAZ width produced with electrode negative [5]. Multiple linear regression model is used to relate convexity index, depth of penetration, reinforcement area, deposition rate and HAZ width to input parameters of GMAW process [6]. Mathematical model is developed for bead geometry relationship for multiple wire SAW process for both DCEP and DCEN [7].

The heat flow condition is significantly affected by change in plate thickness which ultimately affects the bead geometry and strength of weldment. Rosenthal et al. [8] studied that thick plates conduct heat approximately radially in all directions into the plates (3D heat flow) while for thin plates, parallel to plate surface (2D heat flow). For very thin plates, the heat transfer by radiation or convection from the plates also comes in to the picture (2D+R) [8].

Adam [9] presented the equation for 2D heat flow which is shown in (1) where 'T' is Plate temperature (°K), 'K' is thermal conductivity, 'ρ' is Density (Kg/m^3), 'cp' is specific heat of material (J/Kg*°K), 'p' is plate thickness (mm), 'T0' is atmospheric temperature (°K),, 't' is Time (Sec) and 'Ep' is Energy consumed in welding (Joules).

$$\left[\frac{dT}{dt}\right]^{2D} = 2\Pi K \rho c_p \left(\frac{p^2 (T - T_0)^3}{E_p^2}\right) \quad (1)$$

$$\left[\frac{dT}{dt}\right]^{3D} = 2\Pi K \left(\frac{(T - T_0)^2}{E_p}\right) \quad (2)$$

Equation (2) is Rosenthal heat flow equation for thick plates which provides the generalized model for calculating weld cooling rates and considers three dimensional heat flow during

Harish K. Arya is Assistant Professor in Mechanical Engineering Deptt, of Sant Longowal Institute of Engineering & Technology, Longowal Punjab, India (phone: 01672253729; fax: 01672253124; e-mail: arya.iitr@gmail.com).
Kulwant Singh and R. K Saxena are Professor in Mechanical Engineering Deptt, of Sant Longowal Institute of Engineering & Technology, Longowal Punjab, India (e-mail: engrkulwant@yahoo.co.in, ravindra_04@yahoo.com).

welding. Effect of plate thickness on material properties of arc welded steel joints has been investigated and it was found that hardness value decreases as plate thickness decreases and/or distance from weld center line increased [10]. Weighted factor applied to Rosenthal analytical solution for thick and thin plates and found cooling rates for intermediate plate thickness by using HAZ width [11]. Mechanical and microstructural properties are significantly influenced by weld cooling rates especially in range of 800 to 500 °C range. Heat affected zone, weld metal grain size and microstructure affect the toughness of welded joint. Finer grains are obtained with higher cooling rates and low heat input which improves the impact toughness of weldment [12]. Weld cooling rate depends on heat input, material properties, environmental conditions and process variables along with plate thickness of base metal. Efforts are made to experimentally study the effect of these variables on cooling rates and its relevance to weld metal properties for submerged arc welding [13], [14].

III. Plan of Investigation

Base plate was prepared for submerged arc welding by surface grinding and cleaning with acetone. After several experimental trials, ranges of process parameters have been identified and with the help of design expert software, experimental design matrix is prepared. To study the effect of variable plate thickness and various input parameters on bead geometry, various bead parameters like penetration, bead width and reinforcement are measured with microscope with 10x magnification. The adequacy of model developed has been checked with ANAOVA tables generated by design expert software.

IV. Identifying the Process Parameters & Their Limits

Extensive trial runs were carried out to find out the working range of independently controllable input variables for producing sound welding. The upper limit was coded as +2 and the lower limit as -2, the coded values for intermediate values being calculated from the relationship $X_i = 2\left[2X - \left(X_{\max} + X_{\min}\right)\right] / \left(X_{\max} - X_{\min}\right)$, where X_i is the required coded value of a variable and X is any value of variable from $X_{\min}$ to $X_{\max}$; $X_{\min}$ is the lower level of the variable; and $X_{\max}$ is the upper level of the variable. By the trial runs, parameters given in Table I were selected.

TABLE I
Process Parameters and Their Levels

S. No.	Parameters	Units	Symbols	Limits				
				-2	-1	0	+1	+2
1	Current	Amp	*I*	250	275	300	300	325
2	Voltage	Volts	*V*	23	24	25	26	27
3	Welding Speed	m/hr	*S*	20	21.5	22.5	23.75	25
4	Nozzle to plate distance	mm	*N*	18	19	20	21	22
5	Plate thickness	mm	P_{th}	8	10	12	14	16

V. Preparation of Design Matrix

Central composite rotatable factorial (half fraction) design consists of 32 set of coded conditions. It compromises the 2^5 = 24 factorial design plus six center points, one star and one factorial replicate point. All welding variables at the intermediate (0) level constitute the center point and the combination of each of the welding variables at either lowest (-2) or highest (+2) with the other variables at their intermediate levels constitutes the star point. Thus 32 experimental runs allowed the estimation of linear, quadratic and two way interactive effects of the welding variables on bead geometry.

VI. Consumables

ASTM A-516 grade 60 steel is used as base metal for welding. It is a boiler & pressure vessel quality steel which is ideal for moderate and low temperature service. The material is used extensively by industrial boiler and pressure vessel fabrication that provide manufacturing support to the oil, gas and petrochemical industry. This steel has excellent notch toughness and used for LPG storage and transportation tanks. The other variants of steels are EN 10028/P265GH, BS 1501-161-430A, DIN-17155H11. The chemical composition of SA 516 grade 60 is shown in Table II.

TABLE II
Composition of Consumables

Element	Carbon	Manganese	Sulphur	Phosphorus	Ferrous
Base Metal	0.18	0.95	0.008	0.015	rest.
Filler wire	0.13	1.73	0.015	0.016	rest.
Flux	-	1.52	0.015	0.022	rest.

VII. Developing the Design Matrix and Conducting the Experiments

The experiments were conducted as per design matrix to avoid systematic errors of the system. The experiments were performed on Ador tornado 800 submerged arc welding machine. Bead on plate welding has been performed on SA 516 grade 60 plates of size 300 x 150 mm plates. The electrode wire used for the welding was EH 14 (AWS code – F7A2-EH14) of 3.15 mm in diameter. Agglomerated basic flux GEE 541 made by GEE Ltd was used. Table III shows the design matrix for conducting the experiments along with observed values of bead width and penetration.

VIII. Recording the Responses

The welded plates are cut to prepare 10 mm width test specimen. The specimens are polished with various grades of emery papers and itched with 2% Nital solution. The Bead geometry (penetration and bead width) was measured through metallurgical microscope and Metal Power Imaging software for higher accuracy.

State-ease design expert software (Trail Version) has been used to calculate values of the co-efficient for the responses. The ANOVA table for quadratic model for bead width and

penetration has been shown in Tables IV and V respectively.

TABLE III
DESIGN MATRIX

Std No.	Design matrix					*BW*	*P*
	V	*I*	*s*	*N*	*th*		
1.	-1	-1	-1	-1	1	17.41	3.35
2.	1	-1	-1	-1	-1	15.03	3.38
3.	-1	1	-1	-1	-1	17.5	4.62
4.	1	1	-1	-1	1	14.33	4.18
5.	-1	-1	1	-1	-1	17.2	4.27
6.	1	-1	1	-1	1	15.4	2.79
7.	-1	1	1	-1	1	14.18	2.54
8.	1	1	1	-1	-1	14.1	3.45
9.	-1	-1	-1	1	-1	14.7	4.32
10.	1	-1	-1	1	1	16.86	4.95
11.	-1	1	-1	1	1	14.22	2.72
12.	1	1	-1	1	-1	11.7	3.02
13.	-1	-1	1	1	1	14.8	4.92
14.	1	-1	1	1	-1	14.32	4.01
15.	-1	1	1	1	-1	14.44	4.55
16.	1	1	1	1	1	14.32	4.42
17.	-2	0	0	0	0	14.58	4.32
18.	2	0	0	0	0	14.35	4.34
19.	0	-2	0	0	0	13.85	4.31
20.	0	2	0	0	0	14.02	4.12
21.	0	0	-2	0	0	14.28	4.54
22.	0	0	2	0	0	13.5	4.47
23.	0	0	0	-2	0	13.47	3.42
24.	0	0	0	2	0	13.84	3.38
25.	0	0	0	0	-2	16.83	4.12
26.	0	0	0	0	2	12.54	4.04
27.	0	0	0	0	0	16.02	5.57
28.	0	0	0	0	0	13.73	3.66
29.	0	0	0	0	0	13.83	3.72
30.	0	0	0	0	0	12.92	3.82
31.	0	0	0	0	0	13.03	4.42
32.	0	0	0	0	0	14.84	4.57

"+" and "-" show the High and Low levels respectively

TABLE IV
ANOVA TABLE FOR THE QUADRATIC MODEL FOR BEAD HEIGHT

Source	Sum of squares	Df	Mean Square	F value	P value
Model	58.04	9	6.45	62.55	<0.001
A-OCV	11.43	1	11.43	110.83	<0.001
B-Current	2.01	1	2.01	19.47	0.0002
C-Travel Speed	13.77	1	13.77	133.58	<0.001
D-NPD	9.18	1	9.18	89.01	<0.001
AB	0.46	1	0.46	4.49	0.0457
AC	9.33	1	9.33	90.53	<0.001
Residual	2.27	22	0.10		
Lack of Fit	1.90	17	0.11	1.50	0.3467
Pure Error	0.37	5	0.074		
Cor Total	60.31	31			
Std. Dev.	0.32		R^2	0.9624	
Mean	14.57		Adj R^2	0.9470	
C.V. %	2.20		Pred R^2	0.9247	
PRESS	4.54		Adeq Prec	33.195	

TABLE V
ANOVA TABLE FOR THE QUADRATIC MODEL FOR PENETRATION

Source	Sum of squares	Df	Mean Square	F value	P value (Prob. > F)
Model	14.16	12	1.18	30.83	< 0.001
A-OCV	2.61	1	2.61	68.28	< 0.001
B-Current	3.65	1	3.65	95.36	< 0.001
C-Travel Speed	2.60	1	2.60	67.93	< 0.001
D-NPD	1.32	1	1.32	34.38	< 0.001
E-P Thickness	0.78	1	0.78	20.50	0.0002
AC	0.34	1	0.34	8.79	0.0080
AE	0.66	1	0.66	17.14	0.0006
CD	0.22	1	0.22	5.65	0.0281
DE	0.26	1	0.26	6.66	0.0183
Residual	0.73	19	0.038		
Lack of Fit	0.63	14	0.045	2.24	0.1915
Pure Error	0.10	5	0.020		
Cor Total	14.89		R^2	0.9512	
Std. Dev.	0.20		Adj R^2	0.9203	
Mean	4.01		Pred R^2	0.8344	
C.V. %	4.88		Adeq Prec	23.763	
PRESS	2.47				

IX. RESULT AND DISCUSSION

The response function representing any of the weld bead dimension can be expressed as Y = F (V, I, S, N, P_{th}), the relationship selected being a second-degree response surface as per the central composite design. Fig. 1 shows the interaction effect of travel speed and plate thickness on penetration. It was observed that penetration decreases as plate thickness increases which may be due to heat sinking effect in thickness direction. Fig. 2 shows the interaction effect of travel speed and plate thickness on penetration and shows that the reduction in penetration due to heat sinking effect in thickness direction is significant at higher travel speeds. Figs. 3 and 4 show the interaction effect of current and plate thickness on penetration. A significant enhancement of penetration is observed as current value increases, especially with thin plates. Thick plates provide large material below the weld pool to cool molten material faster and hence penetration observed was lesser than expected. Fig. 5 shows the individual effect of each parameter along with plate thickness on bead width and observed that bead width significantly affected by change in voltage but effect of plate thickness was negligible. Fig. 6 shows the interaction effect of travel speed and plate thickness on bead width. Bead width increases with slow travel speed and this improvement was dominating with thin plates. Higher heat input needed for thicker plates for desired bead width.

Equations (3) and (4) show developed model for Penetration and Bead width:

$$P=+4.33+0.33*V+0.39*I-0.3*S+0.23*N-0.18*P_{th} -0.14*V*S-0.20*V*P_{th}+0.12*S*N+0.13*N*P_{th} \quad (3)$$

$$BW=+14.25+0.69*V-0.29*I-0.76*S-0.62*N+0.17*V*I - 0.76*V*S \quad (4)$$

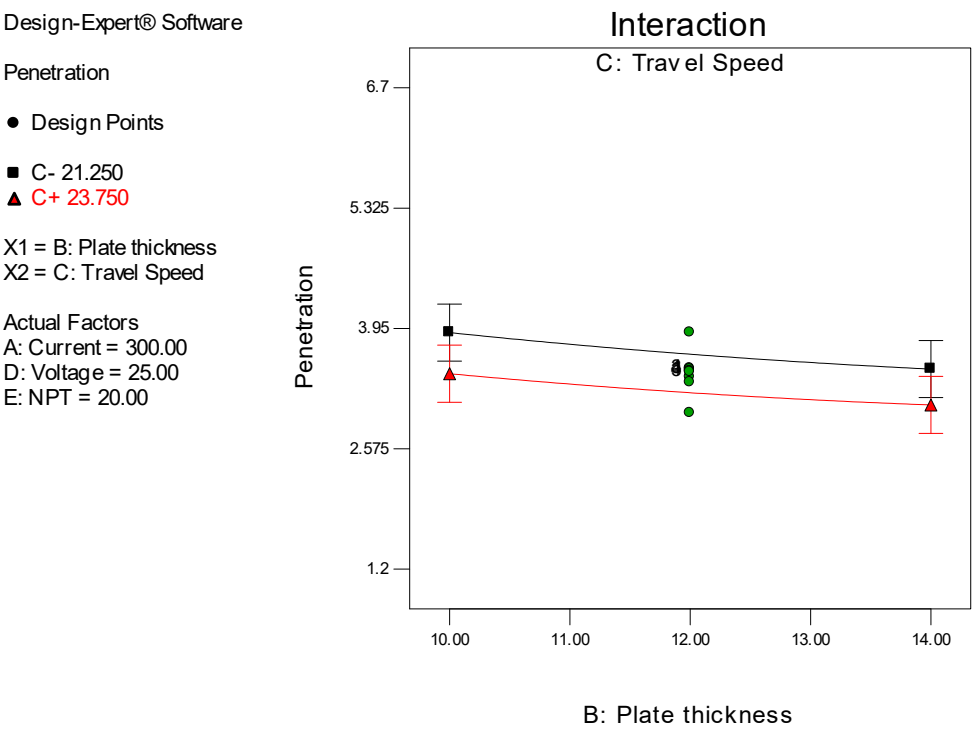

Fig. 1 Interaction effect of travel speed and plate thickness on Penetration

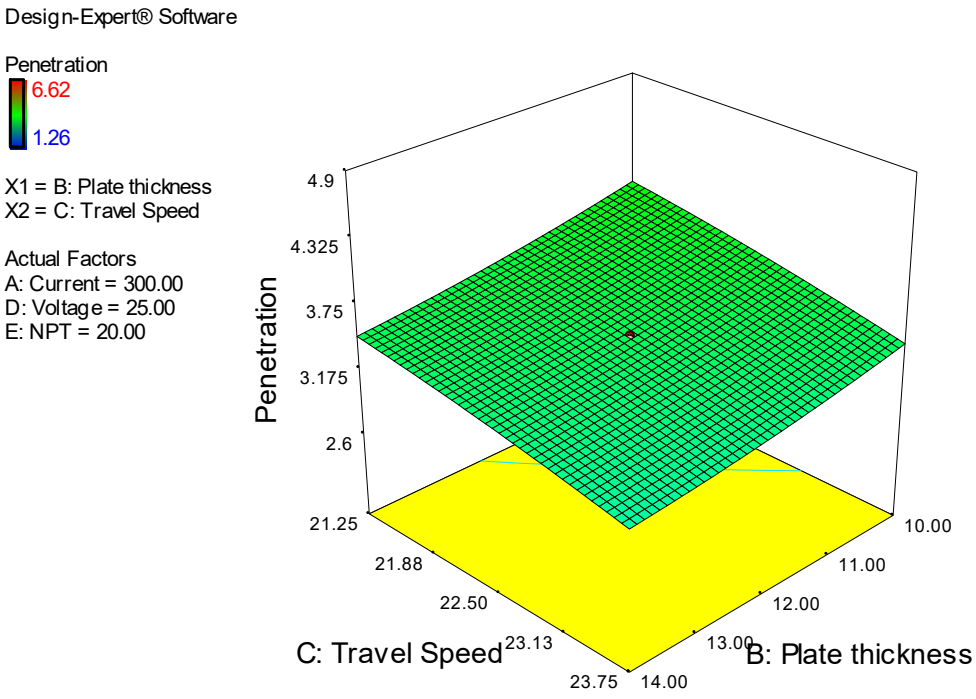

Fig. 2 3D plot for the effect of travel speed and plate thickness on Penetration

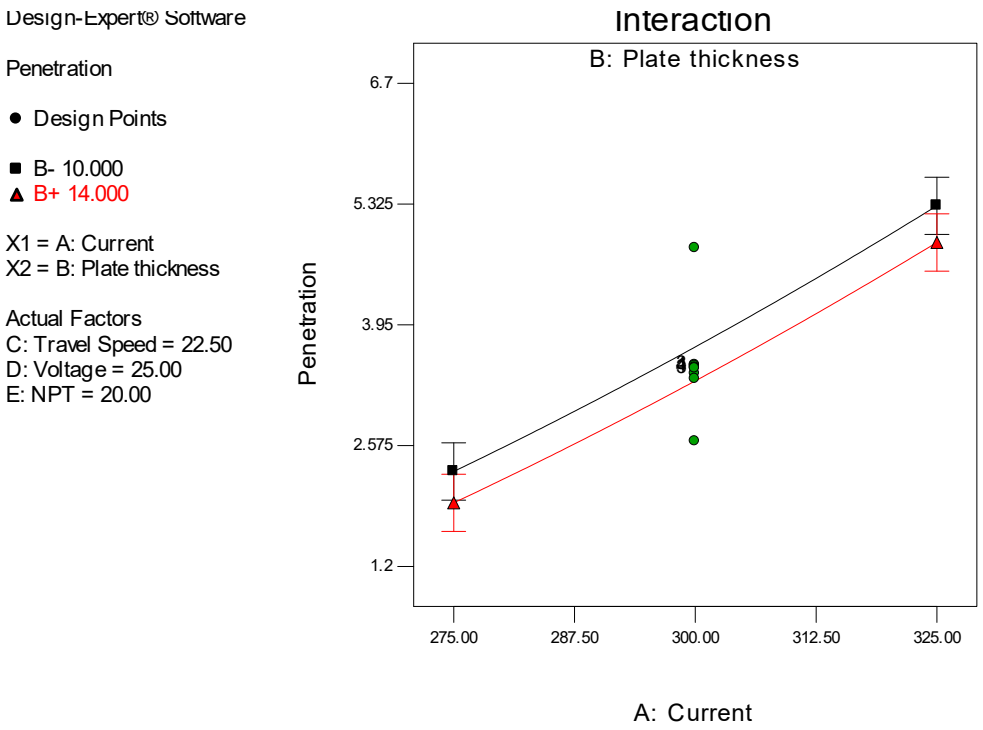

Fig. 3 Interaction effect of current and plate thickness on penetration

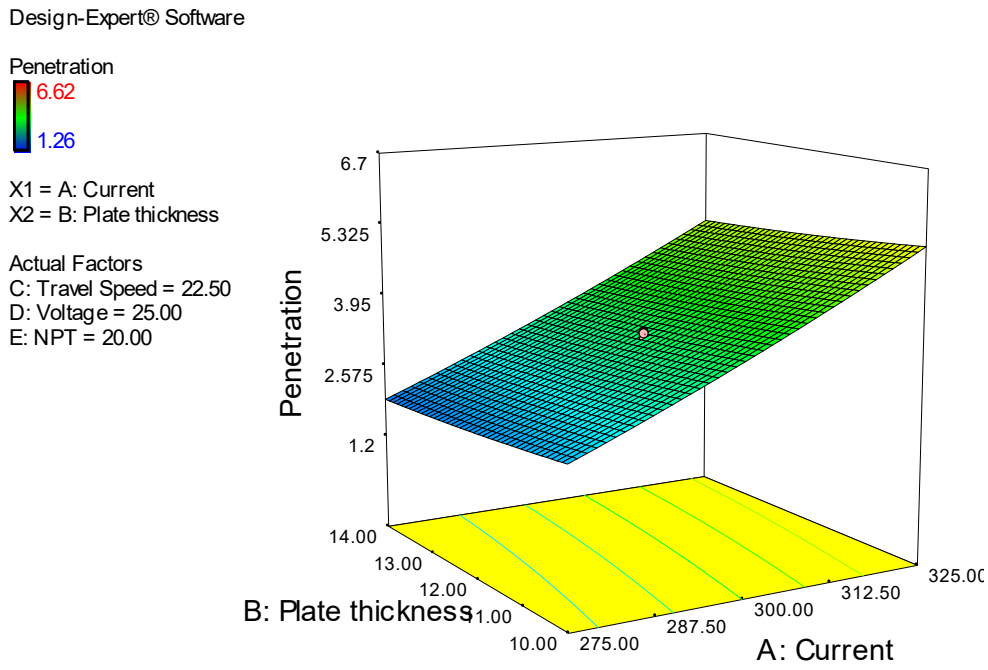

Fig. 4 3D plot of current and plate thickness on penetration

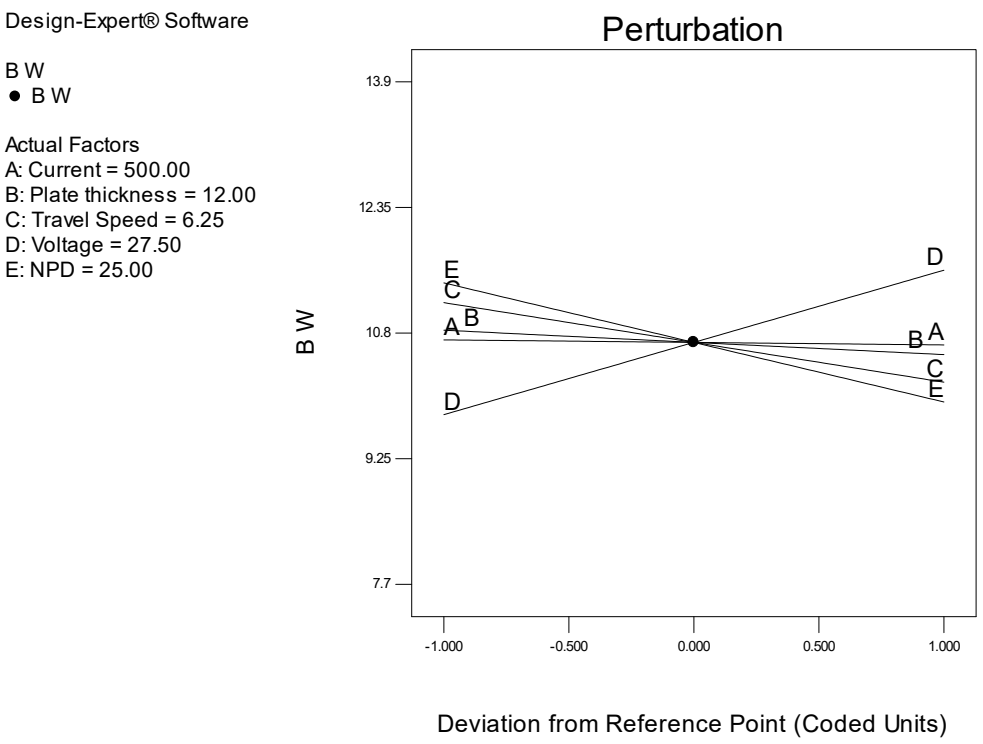

Fig. 5 Effect of various parameters of bead width

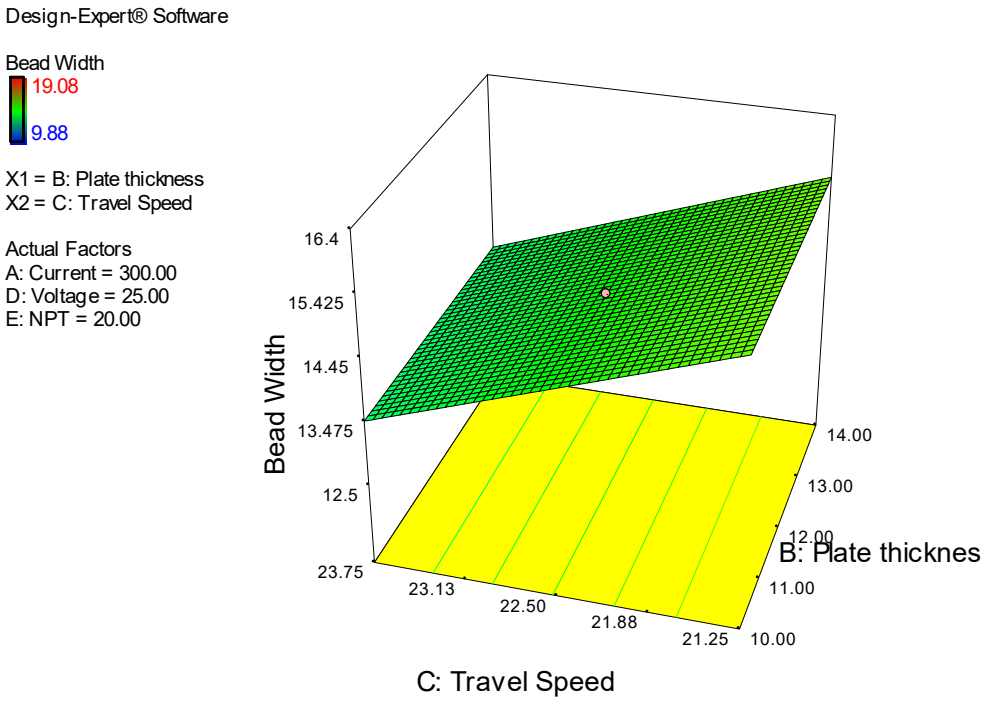

Fig. 6 3D plot for the effect of travel speed and plate thickness on bead width

X. Conclusion

Following conclusions may be drawn from the study:

1. Models to predict penetration and bead width are presented which can be used over wide range of plate thicknesses.
2. Errors in predicting bead parameters due to heat flow conditions are removed and hence models are able to predict with greater accuracy.

3. Penetration increases with current, arc voltage and electrode extension while decreases with plate thickness because the conduction heat loss in thickness direction becomes predominate for thick plates.
4. The weld bead width increases with increase in arc voltage and reduces with welding speed. Minor enhancement in bead width observed with thick plates due to heat sinking in thickness direction.

REFERENCES

[1] V. Gunaraj and N. Murugan, "Application of response surface methodology for predicting weld base quality in submerged AC welding pipes," *Mater. Process. Technol.*, vol. 88, pp. 266–275, 1999.
[2] V. Gunaraj and N. Murugan, "Prediction and comparison of the area of the heat-affected zone for the bead-on-plate and bead-on-joint in submerged arc welding of pipes," vol. 95, pp. 246–261, 1999.
[3] W. Reeta and S. Pandey, "Mathematical models for prediction of weld bead geometry in GMAW of Aluminum alloy 7005," in *ASME Early Career Technical Conference, ASME ECTC Atlanta, Georgia, USA*, 2010, vol. 9, pp. 80–86.
[4] S. Shen, I. N. a. N. A. Oguocha, and S. Yannacopoulos, "Effect of heat input on weld bead geometry of submerged arc welded ASTM A709 Grade 50 steel joints," *J. Mater. Process. Technol.*, vol. 212, no. 1, pp. 286–294, Jan. 2012.
[5] H. OM and S. Pandey, "Effect of heat input on dilution and heat affected zone in submerged arc welding process," *Sadhana*, vol. 38, no. December, pp. 1369–1391, 2013.
[6] D. K. Adak, M. Mukherjee, and T. K. Pal, "Development of a Direct Correlation of Bead Geometry, Grain Size and HAZ Width with the GMAW Process Parameters on Bead-on-plate Welds of Mild Steel," *Trans. Indian Inst. Met.*, 2015.
[7] A. Sharma, N. Arora, and B. K. Mishra, "Mathematical model of bead profile in high deposition welds," *J. Mater. Process. Technol.*, vol. 220, pp. 65–75, 2015.
[8] D. Rosenthal, "Mathematical theory of heat distribution during welding and cutting," *Weld. J.*, vol. 20, no. 5, pp. 220–225, 1941.
[9] J. Adams, C. M., "Cooling rates and peak temperatures in fusion welding," *Weld. J.*, vol. 37, no. 5, pp. 210–215, 1958.
[10] F. Shehata, "Effect of plate thickness on mechanical properties of steel arc welded joints," *Mater. Des.*, vol. 15, no. 2, pp. 105–110, Jan. 1994.
[11] K. Poorhaydari, B. M. Patchett, D. G. Ivey, and Poorhaydari, "Estimation of Cooling Rate in the Welding of Plates with Intermediate Thickness," *Weld. J.*, no. October, pp. 149–155, 2005.
[12] R. Kumar, H. K. Arya, and R. Saxena, "Experimental Determination of Cooling Rate and its Effect on Microhardness in Submerged Arc Welding of Mild Steel Plate (Grade c-25 as per IS 1570)," *J. Mater. Sci. Eng.*, vol. 3, no. 2, pp. 3–6, 2014.
[13] R. K. Saxena and H. Arya, "Effects of welding speed, welding current and plate thickness on temperature variation and angular distortion in butt joint welding," in *Annual International Conference on Materials Science, Metal & Manufacturing (M3 2011) Hotel Fort Canning, Singapore 12th - 13th December*, 2011.
[14] H. Arya, K. Singh, and R. K. Saxena, "Influence of Cooling Rate on Metallurgical Properties of Weld in SAW," in *Annual International Conference on Materials Science, Metal & Manufacturing (M3 2011) Hotel Fort Canning, Singapore 12th - 13th December*, 2011.